

ENERGY GAP ANALYSIS OF $\text{Ba}_{0.25}\text{Sr}_{0.75}\text{TiO}_3$ THIN FILM ON GLASS INDIUM TIN OXIDE (ITO) SUBSTRATE

Rony Febryarto^{1,2 a)}, Novia Fransiska Simbolon^{1 b)}, Dea Widiawati^{1 c)}, Naila Nur Alifa^{1 d)}, Irzaman^{1 e)}

¹Program Studi Fisika, Fakultas MIPA, Institut Pertanian Bogor.

²Badan Riset dan Inovasi Nasional

Email: ^{a)}s3ipb2024rony@apps.ac.id, ^{b)}noviafransiskasimbolon@apps.ipb.ac.id, ^{c)}deawidiawatidea@apps.ipb.ac.id, ^{d)}nailanuralifa@apps.ipb.ac.id, ^{e)}irzaman@apps.ipb.ac.id

Abstrak

Film tipis $\text{Ba}_{0.25}\text{Sr}_{0.75}\text{TiO}_3$ (BST) dibuat pada substrat kaca indium tin oxide (ITO) menggunakan metode deposisi larutan kimia (CSD) diikuti dengan anil. Tujuan dari pekerjaan ini adalah untuk menyelidiki pengaruh doping Rutenium (Ru) pada sifat optik, khususnya energi celah pita, dari film tipis BST. Karakterisasi optik dilakukan menggunakan spektrofotometri UV-Vis dalam rentang panjang gelombang 230–850 nm. Hasilnya mengungkapkan bahwa doping Ru secara efektif memodifikasi struktur elektronik BST, yang mengarah pada pengurangan progresif dalam energi celah pita. Pada substrat silikon, celah pita menurun dari 3,363 eV (*undoped*) menjadi 1,568 eV (1,5% Ru), sementara pada substrat ITO menurun dari 2,116 eV menjadi 1,698 eV untuk tingkat doping yang sama. Tren penurunan ini menunjukkan bahwa Ru memperkenalkan keadaan terlokalisasi atau tingkat cacat dalam struktur BST, yang memfasilitasi transisi elektronik pada energi foton yang lebih rendah. Kemampuan penyetelan celah pita sangat penting untuk aplikasi optoelektronik. Celah pita yang lebih sempit meningkatkan penyerapan cahaya di daerah tampak, yang bermanfaat bagi perangkat seperti sel surya, fotodetektor, sensor optik, dan jendela pintar. Lebih lanjut, kompatibilitas BST dengan oksida konduktor transparan seperti ITO memperkuat potensi integrasinya ke dalam perangkat multifungsi dan hemat energi. Penelitian ini menunjukkan bahwa doping Rutenium memberikan rute yang menjanjikan untuk menyesuaikan celah pita film tipis BST, sehingga memperluas penerapannya dalam teknologi optoelektronik generasi berikutnya.

Kata-kata kunci: $\text{Ba}_{0.25}\text{Sr}_{0.75}\text{TiO}_3$, celah pita, sensor optik.

Abstract

$\text{Ba}_{0.25}\text{Sr}_{0.75}\text{TiO}_3$ (BST) thin films were fabricated on indium tin oxide (ITO) glass substrates using the chemical solution deposition (CSD) method followed by annealing. The objective of this work was to investigate the effect of Ruthenium (Ru) doping on the optical properties, particularly the band gap energy, of BST thin films. Optical characterization was carried out using UV-Vis spectrophotometry in the wavelength range of 230–850 nm. The results revealed that Ru doping effectively modified the electronic structure of BST, leading to a progressive reduction in band gap energy. On silicon substrates, the band gap decreased from 3.363 eV (*undoped*) to 1.568 eV (1.5% Ru), while on ITO substrates it decreased from 2.116 eV to 1.698 eV for the same doping level. This decreasing trend indicates that Ru introduces localized states or defect levels within the BST structure, facilitating electronic transitions at lower photon energies. The tunability of the band gap is highly significant for optoelectronic applications. A narrower band gap enhances light absorption in the visible region, which is beneficial for devices such as solar cells, photodetectors, optical sensors, and smart windows. Furthermore, the compatibility of BST with transparent conducting oxides such as ITO strengthens its potential for

integration into multifunctional and energy-efficient devices. In summary, this study demonstrates that Ruthenium doping provides a promising route to tailor the band gap of BST thin films, thereby expanding their applicability in next-generation optoelectronic technologies.

Keywords: Ba_{0.25}Sr_{0.75}TiO₃, Band Gap, optical sensors,

1. INTRODUCTION

Barium Strontium Titanate or BST is a ceramic that can store electric charge and possesses a very high dielectric constant. BST finds its ubiquitous application in electronics such as capacitors, sensors, and ferroelectric memory devices, due to its features.

Barium Strontium Titanate or Ba_xSr_{((1-x))}TiO₃ refers to barium strontium titanate, which is an essentially mixed compound of BaTiO₃ and SrTiO₃. The ferroelectric Curie temperature (T_c) is dependent on the ratio barium to strontium (the value of x). Pure barium titanate typically has a Curie point at 130 degrees Celsius, but when strontium is added, that temperature drops closer to room temperature (Huriawati and Irzaman, 2015) [1].

Today, BST is commonly used as ultra-thin films grown on a substrate during technology applications. In this way, scientists could easily modify the crystal structure and electrical behavior properties of a material by just adding tiny amounts of different elements also known as dopants. As the demand for advanced materials is exponentially increasing with respect to the fields of optoelectronics and microelectronics, a considerable amount of work has gone into research to develop thin films of BST. One primary reason for this is the availability of wide scalability in the versatility of dielectric and ferroelectric modulation just by changing the barium-to-strontium ratio (Luo et al., 2010)[2].

The chemical formula Ba_{((1-x))}Sr_xTiO₃ describes a solid solution resulting from the mixing of barium titanate with strontium titanate. These two oxides are perovskite-shaped and very well-known in terms of their wide variety of electrical behavior, according to their compositions and processing (Gao et al., 2017) [3].

Indium tin oxide (ITO) is, very simply, a conducting glass that transmits light. Hence, it is an ongoing working electrode for a number of applications in optoelectronics and biosensing, for it permits visible light to pass through while possessing low resistivity. That is why the main interest to deposit barium strontium titanate thin films on indium tin oxide coated glass is that indium tin oxide behaves as a transparent conducting oxide, which is very crucial for applications such as transparent electrodes in solar cells, displays, and several optoelectronic devices (Sun et al., 2021)[4].

In a particular case, the integration of a functional oxide thin film compatible with a transparent conductive oxide substrate, such as barium strontium titanate with ITO, could engender some synergistic effects, which could lead to the possibility of new device functionalities and improved performance characteristics, hence broadening the application scope of these kinds of composite structures. Monitoring energy bandgap in Ba_{0.25}Sr_{0.75}TiO₃ thin films deposited on ITO substrates is critical for understanding their fundamental electronic structure and affecting predictions about their diverse applications at device level in electronic and optoelectronic applications and providing significant results to facilitate advancement and optimizations in device technologies.

Thin films can be fabricated using various deposition techniques, such as sputtering, chemical solution deposition (CSD), or chemical vapor deposition (CVD). These methods work by controlling the reaction rate to achieve film growth on a substrate. They offer advantages including good stoichiometric control, high homogeneity, simple procedures, and low cost (Surono and Sutanto, 2014) [5]. In this paper, we present the synthesis of Ba_{0.25}Sr_{0.75}TiO₃ (BST) thin films doped with different concentrations of Ruthenium using the CSD method, and analyze their optical band gap properties through UV-Vis spectrophotometry to evaluate the effect of doping for optoelectronic applications.

1.1 Synthesis and Characterization Techniques

The UV-Vis spectrophotometer is an instrumental method in chemical analysis used to detect compounds (solid/liquid) based on photon absorbance within the ultraviolet (UV) and visible (Vis) spectrum ranges (Irawan, 2019) [6].

The parameter measured is the absorbance value of the thick BST film. This absorbance value is used to calculate the energy gap. UV-Vis spectroscopy is based on the electronic transitions of organic molecules that absorb light, which excites electrons from lower-energy orbitals to higher-energy orbitals. The energy absorbed at a given wavelength must be equal to the band gap energy. (Rocha et al., 2018) [7].

1.2 Energy Band Gap

The band gap energy of the film was analyzed using the Kubelka-Munk method. The Kubelka-Munk function was employed to determine the band gap energy and to identify the light spectrum sensitivity of the BST film using reflectance data, as described in Equation (1) and Equation (2) (Doyan et al., 2017) [8,12].

$$F(R) = \frac{(1-R)^2}{2R} \propto \alpha_{K-M}$$

$$(\alpha_{K-M} h\nu)^{\frac{1}{\gamma}} = \beta(h\nu - E_g) \quad (2)$$

where R is the reflectance in the absorption region of 230–850 nm, β is a material-dependent constant, γ is the electronic transition factor, h is Planck's constant, ν is the photon frequency, $h\nu$ is the photon energy (in eV), E_g is the optical band gap (in eV), and n equals 2 for indirect transitions and 0.5 for direct transitions.

The determination of the energy bandgap is a critical step in characterizing semiconductor materials, as it influences their suitability for a wide range of applications, including transistors, solar cells, and optoelectronic devices. Therefore, the influence of experimental parameters on semiconductor thin films should be thoroughly analysed.

2. METHODOLOGY

2.1 Substrate Preparation

Prepare p-type silicon (100) substrates and Indium Tin Oxide (ITO) substrates. The silicon substrates are then cut into square pieces measuring 2.5 cm \times 2.5 cm using a diamond-tipped cutter. A total of eight pieces (two replicates) are prepared for four [RuO]₂ doping variations: 0%, 0.5%, 1%, and 1.5%. After cutting, the substrates are weighed using a digital balance. The cut p-type silicon (100) substrates are then washed in a graduated cylinder. The cleaning process consists of five steps: triple rinsing with deionised water (aqua bidest), followed by single rinses with methanol and acetone, respectively.

The process of weighing the ITO substrate is preceded by cleaning. Each cleaning procedure is carried out with the help of an ultrasonic cleaner for 5 minutes per cycle. After cleaning, the substrates are placed on tissue paper and dried with a blower or hand drier. The cleaning is done using deionized water (aqua bidest) five times. The cleaning process is done in an ultrasonic cleaning machine for 10 minutes, with each cycle being 2 minutes long. This cleaning step helps in the removal of impurities or contaminants on the surface of the substrate. Tweezers are used to handle the substrate so that it does not get contaminated. After the substrate is placed on tissue paper, it is dried using a hand drier until completely dry.

Weighting of the dried substrate will be done with a digital balance prior to film coating. This weight shall be referred to as m_1 . The dried, weighed substrates are then put into the compartmentalised storage box consecutively one by one.

2.2 Solution Preparation

With respect to locating another assembly of different fellows, here begins a process of synthesis, which involves preparing materials: substrates of p-type silicon (100), ITO substrates, barium acetate powder, titanium isopropoxide, ruthenium oxide powder, and a solvent consisting of 2-methoxyethanol, deionised water (aqua bidest), acetone, and methanol.

The instruments employed are magnetic stirrer, tweezers, spatula, gloves, mask, digital balance, stir bar, micropipette, tissue paper, spin coater, etc. The reagents are first calculated based on stoichiometric ratios to get a 0.5 M solution, and the required amount of the chemicals was then weighed on a digital balance.

The next step involves weighing 0% dopant variation barium acetate and strontium acetate powdered and then charging it to a vial bottle. Add 4 mL of 2-ethoxyethanol solvent for sample preparation. Stir the samples with the aid of a magnetic stirrer at 500 rpm for 2 hours at a temperature of 40°C .

To this, add titanium isopropoxide and continue stirring for an additional hour. For the 0.5%, 1%, and 1.5% dopants, the same process would be followed as per the undoped solution. When stirring, the dopant is added accordingly, and this is followed by an additional hour of stirring. After this stirring, the solution is filtered with a hydrophilic PVDF filter of porosity 0.45 μm to remove solid particles in turn leaving a much smoother film layer for subsequent use.

TABLE 1. Composition of Materials for BaSrTiO₃ Solution Preparation at 0.5 M Concentration

Dopant Variation	Barium Acetate (g)	Strontium Acetate (g)	Titanium Isopropoxide (mL)	Ruthenium Oxide (g)	2-Methoxyethanol (mL)
0%	0.1276	0.3085	0.5919	-	4
0.5%	0.1276	0.3085	0.5891	0.0013	4
1%	0.1276	0.3085	0.5861	0.0027	4
1.5%	0.1276	0.3085	0.5831	0.0040	4

2.3 Film Fabrication on Substrate

An efficient system for the growth of thin films on substrates has been developed utilizing Chemical Solution Deposition (CSD) and spin-coating techniques. The substrates consist of p-type silicon (100) and ITO. ITO substrates are conductive and may be reversed on either side.

The film was formed by CSD techniques via spin-coating with a 0.5 M solution. Clean and dry substrates were placed onto the spin-coater stage using tapes on double sides. The active side of the ITO surface was to be coated with the solution.

A masking tape was used to mask 0.5 cm on the right and another 0.5 cm on the left of the substrate, leaving the dedicated center area for drop-casting. The three drops of the solution were dropped onto ITO and silicon substrates. There was an interval of 30 seconds between each drop. The spin coater was set at a speed of 3000 rpm for 3 cycles of 30 seconds each. After coating, the substrates were taken off for annealing.

The purpose of the annealing step is to modify enhance properties of the final thin film. This procedure includes heating to an appropriate temperature and maintaining it at that temperature with a controlled cool-off. The sample is placed in a Nabertherm furnace to anneal. A crucible is placed on top of the sample to keep it clean. Temperature rises from room temperature at $[(1.67)]^{\circ}\text{C}$ per minute as per the preset setting. The annealing temperature is given as 550°C for one hour (Bintari, 2022) [9].

From there, the furnace would be maintained at 550°C for another eight hours, followed by a cooling down to room temperature 27°C . The annealing temperature would affect the microstructure, crystal size, crystallinity, lattice parameters, and optical characterizations. The samples undergo several characterizations after being removed from the furnace at lower temperatures (Noviana, 2024) [10].

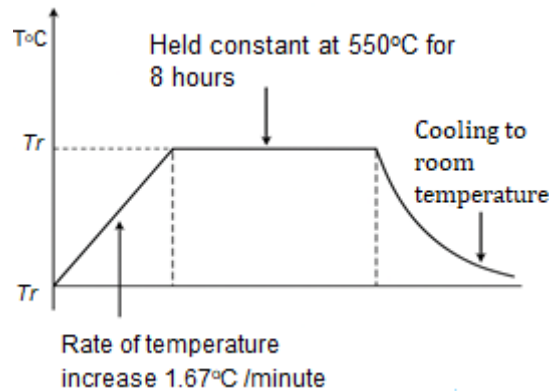


FIGURE 1. Heat treatment profile for the Annealing process

2.4 UV-Vis Spectrophotometer

An optical characterizer (absorbance, reflectance, and transmittance optical features) of a thin film using the UV-Vis optical spectrophotometer (Ocean Optics DH-2000-BAL), has been considered for its characteristics. The UV-Vis spectrophotometer works really well for wavelengths ranging between 200 and 1100 nm. It has a window that goes between 200 and 800 nm (UV portion is between 200 and 400 nm while the visible region stretches from 400 to 800 nm). (Rocha et al., 2018) [7].

A detector, source of light, a sample holder, and a diffraction grating inside the monochromator to separate from amongst other wavelengths of light are the basic parts of a spectrophotometer. The UV-vis spectrophotometer characterization data were then analyzed and processed to quantify reflectance for the test. Through Ultraviolet-Visible tests, a percentage reflectance can be obtained, which is obtained by using an ultraviolet and visible light source. The resulting graph can be plotted as wavelength versus reflectance to evaluate the band gap energy within the film.

3. RESULT

3.1 Optical Characterization

The primary analytical tool for this study was the Ocean Optics USB4000 spectrometer. We conducted a detailed analysis of absorbance and reflectance throughout the UV-Visible spectral range, aiming to clarify the nature of electronic transitions in the films, especially those influenced by changes in photon energy. As we increased the wavelength of the incident light, we observed a clear decline in absorption, a trend that aligns well with previous research (Dewi et al., 2019) [11]. This consistency supports the reliability and reproducibility of the optical behavior seen in BST-based materials.

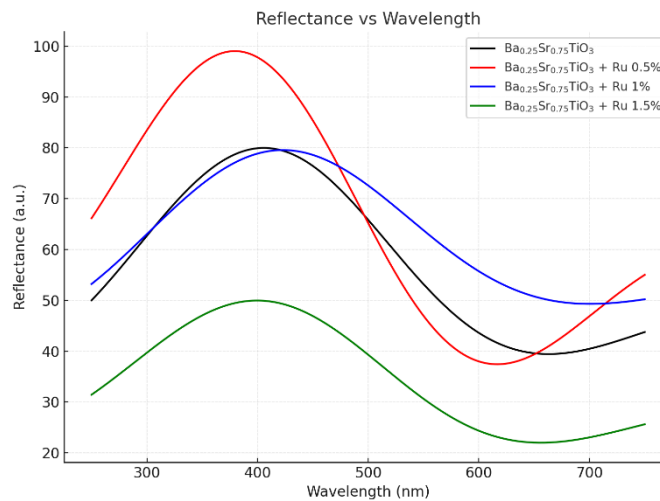


FIGURE 2. Reflectance as a function of wavelength for BaSrTiO₃ thin films doped with different concentrations of Ruthenium on silicon substrates

Figures 2 and 3 show the reflectance spectra of Ba_{0.25}Sr_{0.75}TiO₃ (BST) thin films that have been doped with different concentrations amounts of Ruthenium (Ru). These films were deposited on silicon and indium tin oxide (ITO) substrates. Respectively, there's a clear increase in reflectance values at longer wavelengths, especially in the visible range of the electromagnetic spectrum. This spectral behavior is crucial for estimating the optical band gap energy. To achieve this, the Kubelka-Munk transformation is used to link diffuse reflectance data with absorption coefficients, allowing for a more accurate analysis of the films' electronic structure.

The reflectance behavior affects internally estimated band gap energy. As evident, while the reflectance increases, the energy calculated for the band gap tends to decrease. This suggests an inverse relation: that elevated surface reflectivity is an indication of improved electronic interaction or modified optical transitions occurring in the doped BaSrTiO₃ film.

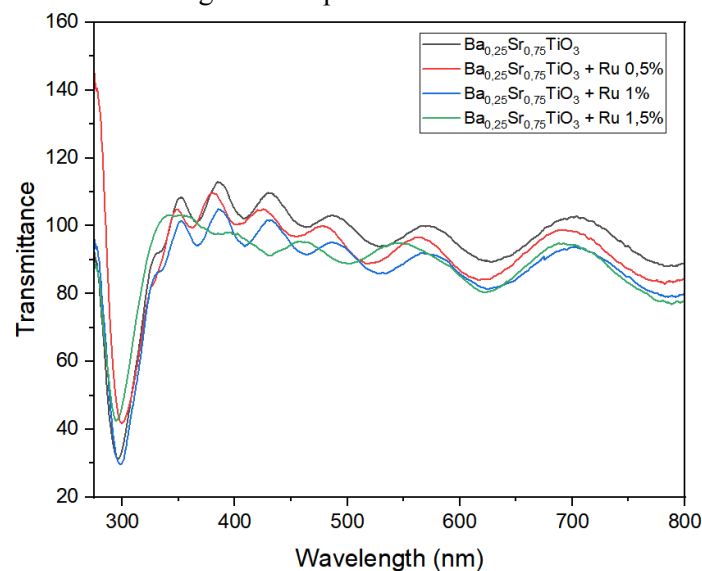


FIGURE 3. Reflectance as a function of wavelength for BaSrTiO₃ thin films doped with different Ruthenium concentrations on ITO substrates

3.2 Band Gap Determination

The bandgap energies of Ba_{0.25}Sr_{0.75}TiO₃ thin films with different doping concentrations of ruthenium (0%, 0.5%, and 1.5%), grown on silicon substrates, were estimated and shown in fig.4. The plot clearly illustrates the decrease of bandgap energy with increasing concentration of ruthenium. The bandgap value for the undoped sample was 3.363 eV, while the two samples with 0.5% Ru doping hardly registered the difference at 3.313 and 3.291 eV, respectively. But, on increasing the doping level to 1.5%, a sharp decrease in the value was observed with the bandgap going down to 1.568 eV.

This decreasing trend indicates that ruthenium doping effectively alters the electronic structure of the BaSrTiO₃ films. The addition of ruthenium probably creates defects or extra energy levels in the band gap, which reduces the energy needed for electronic transitions. This means that the films' ability to absorb light and conduct electricity improves, making them better for use in devices like optoelectronics, photocatalysts, and solar energy systems.

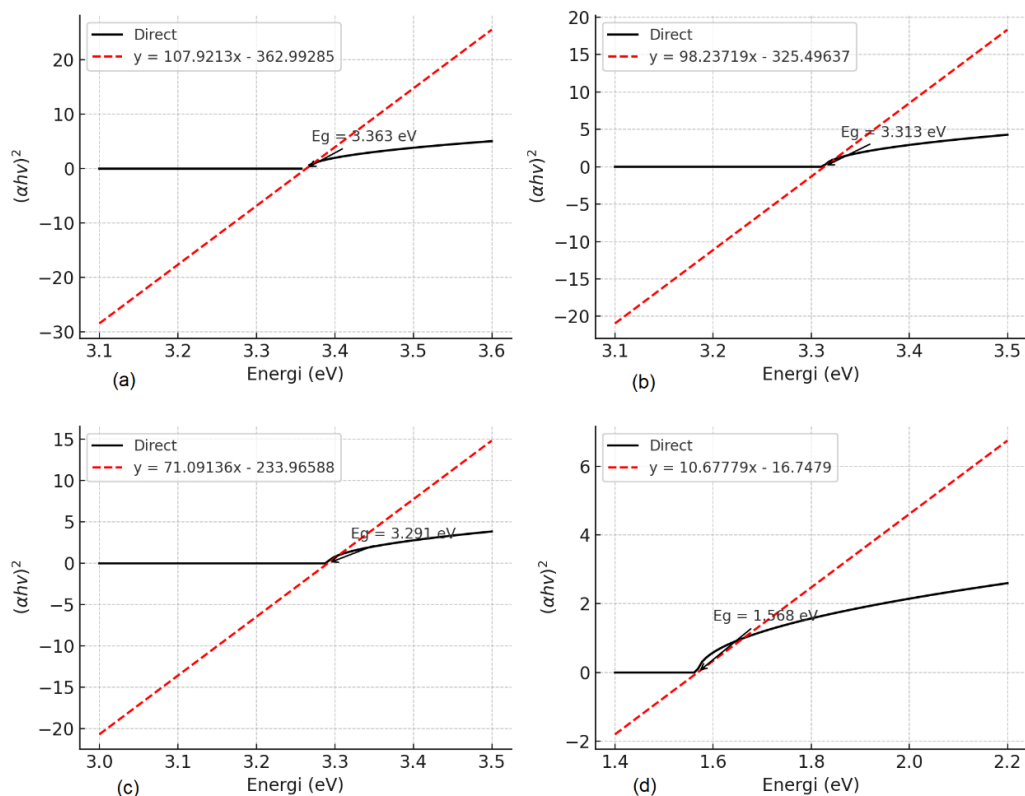


FIGURE 4. Band gap energy values of Ba_{0.25}Sr_{0.75}TiO₃ films doped with Ruthenium at varying concentrations: (a) 0%, (b) 0.5%, (c) 0.5%, and (d) 1.5% on silicon substrates.

These are Figures 5 (a)-(d), Tauc plots useful in establishing the direct band gap energies of the Ba_{0.25}Sr_{0.75}TiO₃ thin films doped with ruthenium in varying amounts: 0%, 0.5%, 0.5%, and 1.5%. Their abscissa plot is $(\alpha h\nu)^2$ vs photon energy ($h\nu$). The value obtained from this was extrapolated from the curves linear portion of the graph traced to the x-axis denoting energy of the band gap (E_g). Accordingly, the values obtained from band gaps are 3.363 eV for undoped film (a), 3.313 and 3.291 eV for 0.5% doped films (b and c), while a very low value at 1.568 eV for the 1.5% doped film (d).

From that, it can be observed that any increase in ruthenium doping concentration reduces the band gap energy of films. This is evidence that the presence of ruthenium introduces states of the kind found in defects or changes the electronic configuration within the material to allow low-energy transitions. The strong drop in band gap at doping 1.5% suggests that a very deep change occurs in the electronic configuration of the material for the reason that it connects with other types to show

greater values for conduction when applications are optoelectronic devices, photocatalysis, or solar energy conversion systems.

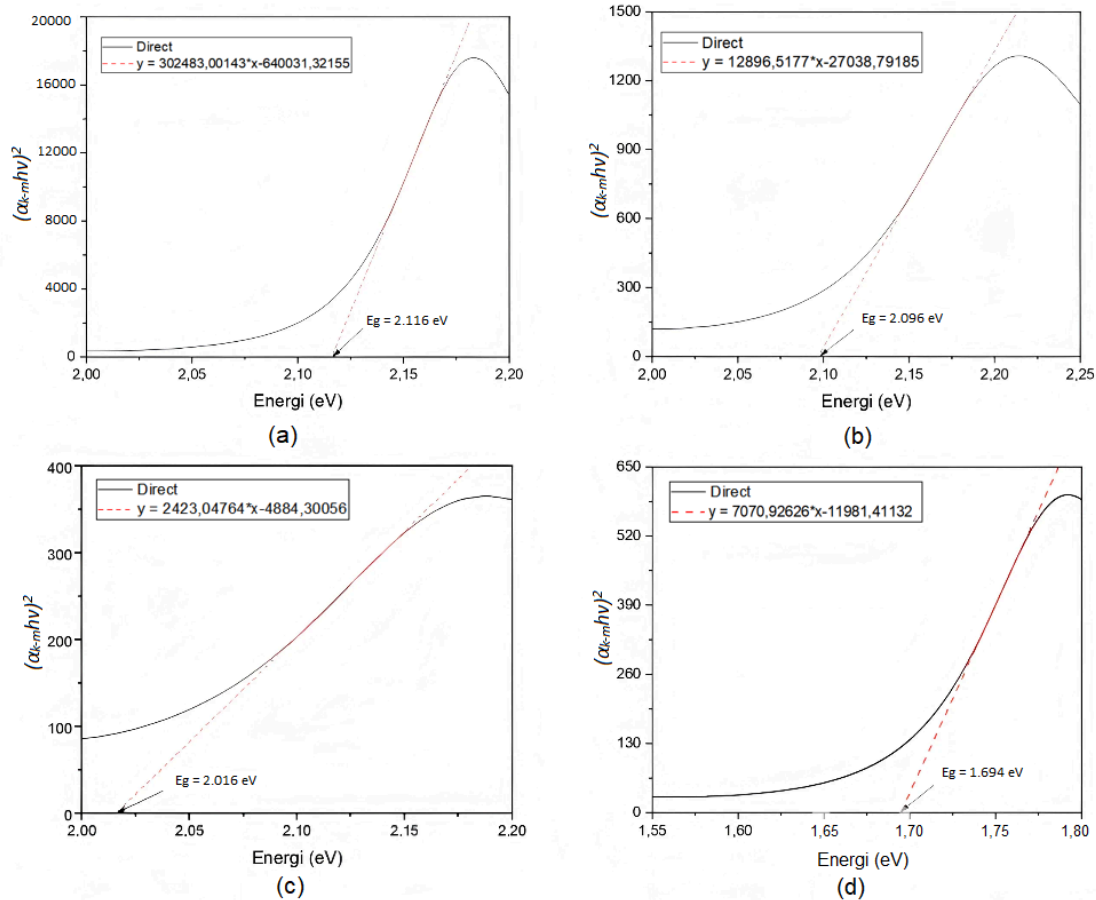


FIGURE 5. Band gap energy values of $Ba_{0.25}Sr_{0.75}TiO_3$ films doped with Ruthenium at varying concentrations: (a) 0%, (b) 0.5%, (c) 0.5%, and (d) 1.5% on ITO substrates.

Table 2 summarizes the band gap energy values of $Ba_{0.25}Sr_{0.75}TiO_3$ thin films doped with different concentrations of Ruthenium Ru on various substrates: silicon, ITO. The undoped $Ba_{0.25}Sr_{0.75}TiO_3$ film shows a band gap energy of 3.363 eV on a silicon substrate and 2.116 eV on an ITO substrate.

TABLE 2. Composition of Materials for $BaSrTiO_3$ Solution Preparation at 0.5 M Concentration

Ruthenium Dopant Variation (%)	Energi bandgap Silicon Substrate(eV)	Energi bandgap ITO Substrate (eV)
$Ba_{0,25}Sr_{0,75}TiO_3$	3.363	2.116
$Ba_{0,25}Sr_{0,75}TiO_3 + Ru 0,5\%$	3.313	2.096
$Ba_{0,25}Sr_{0,75}TiO_3 + Ru 1\%$	3.291	2.016
$Ba_{0,25}Sr_{0,75}TiO_3 + Ru 1,5\%$	1.568	1.698

Barring further ru doped concentrations, the general decrease in energy band gap for both silicon and ITO substrates has been seen to trend from 1.5% up to 0.5% concentrations of Ru dopant. Small reductions in band gap are evidenced with low dopant concentrations: 3.291 eV on silicon and 2.016 eV on ITO at 1% Ru. There is a significant reduction observed at 1.5% Ru doping: the band gap drops to 1.568 eV on silicon and 1.698 eV on ITO. This sharp decrease at higher doping concentration suggests that Ruthenium may act an dopant in modifying the electronic structure of $BaSrTiO_3$ by narrowing the band gap significantly.

4. CONCLUSION

The reflection values are mainly noticed from the visible light region, with the Kubelka-Munk function employed to estimate the optical band-gap energy. The optical characterization using UV-Vis spectrophotometry revealed that the band gap energy of $\text{Ba}_{0.25}\text{Sr}_{0.75}\text{TiO}_3$ (BST) thin films can be significantly reduced by Ruthenium doping. The band gap decreased from 3.363 eV (undoped) to 1.568 eV (1.5% Ru) on silicon substrates, and from 2.116 eV to 1.698 eV on ITO substrates.

This reduction indicates that Ruthenium effectively modifies the electronic structure of BST, enabling the material to absorb photons with lower energy. Such tunability in the band gap is crucial for optoelectronic applications, including solar cells, photodetectors, and optical sensors, as it broadens the absorption range within the visible spectrum.

Therefore, Ruthenium doping provides a promising route to engineer and tailor the band gap of BST thin films, enhancing their potential for multifunctional device applications. Future research should focus on optimizing doping levels to achieve the most desirable optical and electronic properties for specific device implementations.

The decreasing trend in band-gap energy with increasing concentration of the dopant was observed quite well in silicon and ITO substrates. The change was very little between 0% and 1% while a sharp fall was recorded at 1.5% doping. This indicates that the electronic structure of the material is altered with the Ru doping, which then influences the optical absorption characteristics.

Nevertheless, doping Ruthenium into $\text{Ba}_{0.25}\text{Sr}_{0.75}\text{TiO}_3$ thin films is an important means of creating an adjustable optical band gap. This tunability is important to maximize the structures for optoelectronic applications such as solar cells and optical sensors. Future work will probably entail optimizing the dopant levels such that the obtained optical and electronic properties become relevant for the implementations in devices.

REFERENCE

- [1] Huriawati F and Irzaman "Kajian Sifat Optik Film Tipis BST didadah niobium dan tatalum" *JPFK*. 2015 **1** (1) 9-13
- [2] Luo J, Yang X Y and Li D L "Preparation of TiO_2 Nanoparticles Doped with Cs^+ and Sr^{2+} and Their Photocatalytic Activity under Solar Light" *Advanced Materials Research* 2010 **113-116** 1945-1950 <https://doi.org/10.4028/www.scientific.net/amr.113-116.1945>
- [3] Gao J, Xue D, Liu W, Zhou C and Ren X "Recent Progress on BaTiO_3 -Based Piezoelectric Ceramics for Actuator Applications" *Actuators* 2017 **6**(3) 24 <https://doi.org/10.3390/act6030024>
- [4] Sun Y, Liu T, Kan Y, Gao K, Tang B and Li Y "Flexible Organic Solar Cells: Progress and Challenges" *Small Science*. 2021 **15** <https://doi.org/10.1002/smssc.202100001>
- [5] Surono A T and Sutanto H "Sifat optik zinc oxide (ZnO) yang dideposisi di atas substrat kaca menggunakan metode chemical solution deposition (CSD) dan aplikasinya untuk degradasi zat warna methylene blue". 2014 *Youngster Phy. J.* **2**(1) 7-14
- [6] Irawan A "Kalibrasi spektrofotometer sebagai penjaminan mutu hasil pengukuran dalam kegiatan penelitian dan pengujian" *Indonesian J. Laboratory* 2019 **1**(2) 1-9
- [7] Rocha F S, Gomes A J, Lunardi C N, Kaliaguine S and Patience G S "Experimental methods in chemical engineering: ultraviolet visible spectroscopy-UV Vis" *Canadian Journal of Chemical Engineering* 2018 **96**(1) 2512-2517 <https://doi.org/10.1002/cjce.23344>
- [8] Doyan A and Humaini "Sifat optik lapisan tipis ZnO " *Jurnal Pendidikan Fisika dan Teknologi*. 2017 **3**(1) 34-39
- [9] Putri L B, Vania R, Palupi E K, Patonah N, Irmansyah, Sumaryada T and Irzaman "Effect of Light Intensity on Magnetic Properties of SrTiO_3 Thin-Films" *Key Engineering Material*. 2020 **855** 208-212

- [10] Noviana R A "Uji sifat kristal dan optik film tipis barium stronsium titanat ($Ba_{0,4}Sr_{0,6}TiO_3$) didadah cuprum (II) asetat ($Cu(CH_3COO)_2$)" *Undergraduate thesis* 2024 (Bogor: IPB University)
- [11] Dewi R, Krisman, Khaironiati and Fauzina "Karakterisasi mikrostruktur material feroelektrik $Ba_{0,8}Sr_{0,2}TiO_3$ (BST) dengan variasi suhu annealing." *Jurnal Fisika Indonesia* 2014 **53**(18) 70-72
- [12] Bajpai P 2018 *Biermann's Handbook of Pulp and Paper: Paper and Board Making* (3rd edn, volume 2) 237-271 (Amsterdam: Elsevier)
- [13] Nurhidayah, Samidar, Frastica D, Mardian P, Anggraini R M, Afrianto M F, Irzaman, Dahrul M, Meilini R, Anis M R, and Ridwan S "Synthesis and Characterization of Lithium-doped $BaTiO_3/Si(100)$ Thin Films with Variations of 0 %, 0.5 %, 1 % and 1.5 % as Potential Forerunners of Solar Cells" *International Journal of Nanoelectronics and Materials* 2024 **17** (1) <https://doi.org/10.58915/ijneam.v17i1.503>
- [14] Sirait N, Motlan and Siregar N "Pengaruh Doping SBCL3 Terhadap Struktur dan Sifat Optik Film Tipis ZNO Dengan Metode Sol-gel Spin Coating" *Einstein e-Journal* 2021**9**(1) 8-15
- [15] Mustafa H A and Jameel D A "Modeling and the main stages of spin coating process: A review". *Journal of Applied Science and Technology Trends* 2021 **2**(3) 91-95
- [16] Al-Ahmadi N A "Metal oxide semiconductor-based Schottky diodes: a review of recent advances" *Material Research Express* 2020 **7**(3) 016401 <https://doi.org/10.1088/2053-1591/ab7a60>
- [17] Ihwani S A " Pengaruh Fraksi-X Selenium pada Struktur dan Parameter Kisi Pb(S,Se) Masif Preparasi Teknik Bridman". *Jurnal Ilmu Fisika dan Terapannya*. 2022**9**(2) 1-13
- [18] Dewi R, Krisman, Zulkarnaen Z, Syahraini R A and Husein T L "The Determination of Barium Strontium Titanate Thin Film Band Gap Energy $Ba_{0,15}Sr_{0,85}TiO_3$ Using Ultraviolet-Visible Spectroscopy" *Spektra: J. Fis. Aplik.* 2020**5**(1) 11-20 <https://doi.org/10.21009/SPEKTRA.051.02>
- [19] Vigneshwaran B, Kuppusami P and Ajith Kumar S "Structural and optical properties of $Ba_{0,5}Sr_{0,5}TiO_3$ thin films on single crystalline substrates" *Materials Science in Semiconductor Processing* 2022 **148** 106795 <https://doi.org/10.1016/j.mssp.2022.106795>
- [20] Dewi R, Manalu W A, Asrinaldo B N, Rini A S and Yanuar Y "Characterization Of Energy Band Gap Thin Film $BaTiO_3/BaZr_{0,5}Ti_{0,5}O_3$ Using Diffuse Reflectance Spectroscopy (DRS) Method" *Spektra: Jurnal Fisika dan Aplikasinya*. 2023 **8**(1) 17-24 <https://doi.org/10.21009/SPEKTRA.081.02>
- [21] Andrade P H M et al. "Band gap analysis in MOF materials: Distinguishing direct and indirect transitions using UV-Vis spectroscopy" *Applied Material Today*. 2024 **37** 102094 <https://doi.org/10.1016/j.apmt.2024.102094>
- [22] Liu Y, Sirui Li, Fausto G, and Evgeny V R "Sol-gel synthesis of tetragonal $BaTiO_3$ thin films under fast heating" *J. Applied Surface Science* 2024 **661** 16006 <https://doi.org/10.1016/j.apsusc.2024.160086>
- [23] Alireza R, Hossein A and M Reza G "Optical properties of multi-stacked $BaTiO_3/SrTiO_3$ thin films" *Ceramic International* 2021 **47** 17895-17906 <https://doi.org/10.1016/j.ceramint.2021.03.102>
- [24] Maryam G E, Abdelrahman M M, Moustafa G and Sameh O A "Optical investigation and computational modelling of $BaTiO_3$ for optoelectronic devices applications" *Scientific Reports* 2023 **10036486** 36959231 doi: 10.1038/s41598-023-31652-2
- [25] C Rios, L Bazan D, Christian A C, Salcedo R and Thangarasu P "Synthesis and Characterization of a Photocatalytic Material Based on Raspberry-like $SiO_2@TiO_2$

- Nanoparticles Supported on Graphene Oxide” *Molecules* 2023 **28** (21) 7331 doi: 10.3390/molecules28217331
- [26] Boubaia A, Assali A, Berrah S, Bennacer H, Zerifi I and Boukortt A “Band gap and emission wavelength tuning of Sr-doped BaTiO₃ (BST) perovskites for high-efficiency visible-light emitters and solar cells.” *Materials Science in Semiconductor Processing* 2021 **130** 105837 <https://doi.org/10.1016/j.mssp.2021.105837>
- [27] Irzaman, Rahmawaty V, Palupi E K, Patonah N, Sumaryada T, Siskandar R, Alatas H, Iqbal M, B Yulianto, M Z Fahmi, Rusydi F and Nugroho W S “The effect of photoconductive mole fraction based on thin film Ba_xSr_{1-x}TiO₃ (X = 0.000; 0.125; 0.250; 0.375; 0.500) on electrical properties and diffusivity coefficient” *Biointerface Research in Applied Chemistry* 2021 **11**(6) 14956–14963 <https://doi.org/10.33263/BRIAC116.1495614963>
- [28] Irzaman, Dahrul M, Rahmani M, Rukyati A M, Samsidar, Nurhidayah, Deswardani F, Peslinof M, Jenie R P, Iskandar J, Wahyuni Y, Priandana K and Siskandar R “Design and fabrication of photovoltaics based on MFS (Ag/BaTiO₃/Si(100) p-type) structure” *Materials Science for Energy Technologies*. 2024 **7** 29-34 <https://doi.org/10.1016/j.mset.2023.06.002>